

# A Simple Blass Matrix Design Strategy for Multibeam Arbitrary Linear Antenna Arrays

Giulia Buttazzoni<sup>1</sup>, Senior Member, IEEE, Elena Marongiu, Student Member, IEEE, Alessandro Fanti<sup>1</sup>, Senior Member, IEEE, Andrea Melis, Nicola Curreli<sup>1</sup>, Member, IEEE, Santi Concetto Pavone<sup>1</sup>, Senior Member, IEEE, Gino Sorbello<sup>1</sup>, Member, IEEE, Giovanni Maria Schettino, Francesca Vatta<sup>1</sup>, Member, IEEE, Fulvio Babich<sup>1</sup>, Senior Member, IEEE, and Massimiliano Comisso<sup>1</sup>, Member, IEEE

**Abstract**—Multibeam antenna arrays are currently recognized as one of the enabling technologies for the next-generation communication standards. One of the key components of these systems is the beamforming network (BFN) that implements the array element excitations. This article addresses this issue by presenting a novel strategy to realize an analog feeding network, which allows an arbitrary linear array (LA) to radiate

multiple arbitrary beams. In particular, an iterative procedure is conceived to design a Blass matrix using an identical directional coupler for all nodes, resulting in a very simple structure suitable for large-scale production. Two applications with arbitrary directions are illustrated as proofs-of-concept for the developed architecture: a dual-beam configuration with a null involving an aperiodic LA, and a four-beam configuration involving a periodic LA. For this second application, the effectiveness of the proposed solution is further verified by full-wave simulations and experimental measurements carried out on a fabricated prototype.

**Index Terms**—Analog beamforming, Blass matrix, feeding network, multibeam antennas.

Manuscript received 6 March 2023; revised 26 July 2023; accepted 23 August 2023. Date of publication 5 September 2023; date of current version 30 October 2023. This work was supported in part by the Sardegna Ricerca-Regione Autonoma della Sardegna—Programma Regionale di Sviluppo 2020–2024, in part by the Strategia 2—Identità economica, in part by the Progetto 2.1—Ricerca e Innovazione Tecnologica, in part by the Research and Development Program Information and Communication Technologies (ICT) through “SAURON5G” Contract under Grant Unique Project Code (CUP) F23D23000170002, in part by the framework of the Project eINS-Ecosystem of Innovation for Next Generation Sardinia under Grant ECS 00000038, in part by the Italian Ministry for Research and Education (MUR) under the National Recovery and Resilience Plan (PNRR)—MISSION 4 COMPONENT 2, “From research to business” INVESTMENT 1.5, “Creation and Strengthening of Ecosystems of Innovation,” and construction of “Territorial Research and Development Leaders,” and in part by the Italian Ministry of University and Research (MUR) through the Project FRA 2023 (University of Trieste, Italy), under Grant D13-FRA-23. (Corresponding author: Giulia Buttazzoni.)

Giulia Buttazzoni, Francesca Vatta, Fulvio Babich, and Massimiliano Comisso are with the Department of Engineering and Architecture (DIA), University of Trieste, 34127 Trieste, Italy, and also with the National Inter-University Consortium for Telecommunications (CNIT), 50139 Florence, Italy (e-mail: gbuttazzoni@units.it; vatta@units.it; babich@units.it; mcomisso@units.it).

Elena Marongiu and Andrea Melis are with the Department of Electrical and Electronic Engineering (DIEE), University of Cagliari, 09123 Cagliari, Italy (e-mail: e.marongiu10@studenti.unica.it; andrea.melis89@unica.it).

Alessandro Fanti is with the Department of Electrical and Electronic Engineering (DIEE), University of Cagliari, 09123 Cagliari, Italy, and also with the National Inter-University Consortium for Telecommunications (CNIT), 50139 Florence, Italy (e-mail: alessandro.fanti@unica.it).

Nicola Curreli is with the Functional Nanosystems, Italian Institute of Technology (IIT), 16163 Genoa, Italy, also with the Transport at Nanoscale Interfaces Laboratory, Swiss Federal Laboratories for Materials Science and Technology (Empa), 8600 Dübendorf, Switzerland, and also with the Molecular Foundry, Lawrence Berkeley National Laboratory, Berkeley, CA 94720 USA (e-mail: nicola.curreli@iit.it).

Santi Concetto Pavone and Gino Sorbello are with the Department of Electrical, Electronics, and Computer Engineering (DIEE), University of Catania, 95125 Catania, Italy (e-mail: santi.pavone@unict.it; gino.sorbello@unict.it).

Giovanni Maria Schettino is with the Department of Engineering and Architecture (DIA), University of Trieste, 34127 Trieste, Italy (e-mail: giovannimaria.schettino@studenti.units.it).

## I. INTRODUCTION

THE basic idea of combining multiple antennas into a single array to improve the electromagnetic performance of a single element dates back to the very beginning of wireless communication history [1]. In fact, over the last century, a huge number of synthesis methods have been developed to satisfy a wide variety of constraints [2], [3]. Therefore, beamforming, in its massive multiple-input multiple-output (mMIMO) context, is nowadays regarded as one of the “big-three” enabling technologies for the forthcoming fifth- and sixth-generation (5G/6G) ecosystems [4], [5]. Among the possible applications, such as reconfigurability, scanning, beam/null steering, and multidirectional coverage, the latter one is expected to play a key role in increasing the 5G/6G capacity and fostering the interoperability among the terrestrial, aerial, and spatial 6G layers [6], [7]. In this context, the capability of multibeam antennas to cover multiple angular regions, thus enabling spatial multiplexing and multitarget tracking, requires not only a careful design of the array structure in terms of a single radiator and geometry, but also specific attention to the realization of the beamforming network (BFN) implementing the selected excitations.

### A. Related Work

The current techniques for designing BFNs primarily rely on either digital electronic platforms [8] or analog microwave components [9], although hybrid solutions have also been explored [10]. The digital approach offers greater versatility, but is also more expensive and power-consuming. Thus, the

interest of 5G/6G industry manufacturers in large-scale low-cost equipment seems mainly oriented toward the analog approach [11]. Cheap and efficient microwave solutions are represented by the so-called “circuit-type” BFNs, which consist of basic components, such as power dividers, couplers, crossovers, phase shifters, and switches. Among them, the Blass [12], [13], [14], [15], [16], [17], [18], [19], Nolen [20], [21], and Butler matrices [22], [23], [24] are the most widely diffused technologies.

The first of these techniques, conceived by Blass in [12], represents the pioneering proposal for analog BFNs supporting multidirectional uniform linear arrays (ULAs). The Blass matrix, whose design requires a proper account for the coupling among waves traveling in different lines [13], has the advantage of being suitable for any number  $N$  of array elements and any number  $M$  of arbitrarily shaped beams. This leads to very versatile structures, which are easier to build in some particular cases, such as when double or uniformly spaced beams are desired [14], [15]. A recent advance enabling independent beam control has been proposed in [16], by adopting generalized joined coupler matrices and particle swarm optimization to allow a systematic BFN synthesis, further modifying the original Blass configuration by placing the phase shifters on the rows instead of on the columns. It is worth noting that this latter modification was originally proposed in the earlier work of Cummings [25]. A multibeam algorithm for evaluating the phase shifts of a simplified Blass matrix with identical couplers has been presented in [17] and subsequently exploited in [18] to numerically derive a preliminary BFN design with dummy antennas. In general, the main disadvantages of the Blass approach lie in its high number of components (couplers and phase shifters) and its inherently lossy nature, due to the need of terminating rows and columns on matched loads. To deal with this issue and simplify the typical architecture, a modified Blass matrix design has been presented in [19], where some components have been removed, but at the cost of limiting the array size and the number of obtainable beams. A more general technique to address the same problem relies on the adoption of a series-fed BFN, called Nolen matrix [20], [21]. This structure, which is regarded as a lossless variant of the Blass one, unfortunately is less flexible, due to the orthogonality constraint resulting from the lossless requirement (this is the same as with Butler matrices). In addition, it can synthesize only  $N = M$  orthogonal beams, hence leading to a considerable flexibility reduction compared to the Blass approach. This constraint also affects the Butler matrix [22], which is a parallel-fed BFN characterized by well-established design procedures [23], [24], and a theoretical absence of losses. However, its pattern control capability is limited since  $N = M$  must be a power of two, and the amplitude distribution at the antenna terminals must be uniform. The limitations imposed by the lossless design on the number of beams and antennas have been widely recognized so that over the years, many researchers have tackled the problem. Interestingly, a Nolen matrix proposal having  $M < N$  and maintaining its lossless nature in transmitting mode has been developed and discussed in [26], however, it is lossy in the receiving mode.

Shelton and Kelleher [27] discussed the limitation of the traditional Butler matrices employing hybrid couplers ( $N = M = 2^b$ ) and proposed the usage of more complex junctions allowing also other configurations (e.g.,  $3 \times 3$ ).

## B. Motivation and Contribution

In terms of design efforts, Butler BFNs are the easiest to realize since they rely on identical hybrid couplers. On the other hand, the Blass and Nolen BFNs require a larger number of unbalanced couplers, whose technology must be carefully selected to achieve the necessary coupling range [11]. In terms of construction complexity, the Blass and Nolen BFNs adopt a higher number of phase shifters than those used by the Butler matrix, whose implementation, however, requires a large number of crossovers. This leads to a multilayer design, which is more laborious to realize than the Blass and Nolen planar structures, and is also inherently lossy because of the layer transitions. In terms of flexibility, the Blass BFN is the sole able to manage problems involving arrays with any number of elements required to generate any number of arbitrarily oriented beams. As a consequence, the derivation of planar Blass matrix evolutions that achieve a satisfactory versatility/complexity tradeoff may represent an interesting advance for the realization of low-cost antenna systems.

To address this issue, this article proposes a systematic Blass matrix design procedure for arbitrary linear arrays (ALAs) generating multiple arbitrary beams. The BFN architecture is planar and adopts identical directional couplers, making the structure very simple. It relies on a properly developed iterative method for the estimation of the phase shifters, which accounts for the wave multipath within the network. With respect to the preliminary studies in [17] and [18], the solution presented here generalizes the design to ALAs supporting multiple independent beams with nulls. Additionally, it includes full-wave simulations and presents experimental measurements derived from a fabricated array-BFN planar prototype.

The article is organized as follows. Section II describes the addressed problem. Section III presents the developed procedure. Section IV discusses the numerical and experimental results. Finally, Section V summarizes the main conclusions.

## II. PROBLEM DESCRIPTION

With reference to a Cartesian system  $O(x, y, z)$ , let us consider an ALA consisting of  $N$  elements lying on the  $z$ -axis at positions  $z_n$ , where  $n \in \mathcal{N} = \{n | n = 1, \dots, N\}$ , which has to radiate  $M$  beams in arbitrarily selected directions. To perform this task, a synthesis algorithm is adopted to calculate the  $M \times N$  matrix  $\mathbf{A} = [a_{mn}]$ , where  $m \in \mathcal{M} = \{m | m = 1, \dots, M\}$ , and the  $m$ th row  $\mathbf{a}_m = [a_{m1}, \dots, a_{mN}]$  identifies the complex array excitations that generate the electric far-field pattern

$$R(\mathbf{a}_m; \theta) = \sum_{n=1}^N a_{mn} f_n(\theta) \exp\left(j \frac{2\pi}{\lambda} z_n \cos \theta\right) \quad (1)$$

where  $\theta$  is the zenith angle,  $f_n(\theta)$  is the  $n$ th element pattern,  $j = \sqrt{-1}$  is the imaginary unit, and  $\lambda$  is the free-space

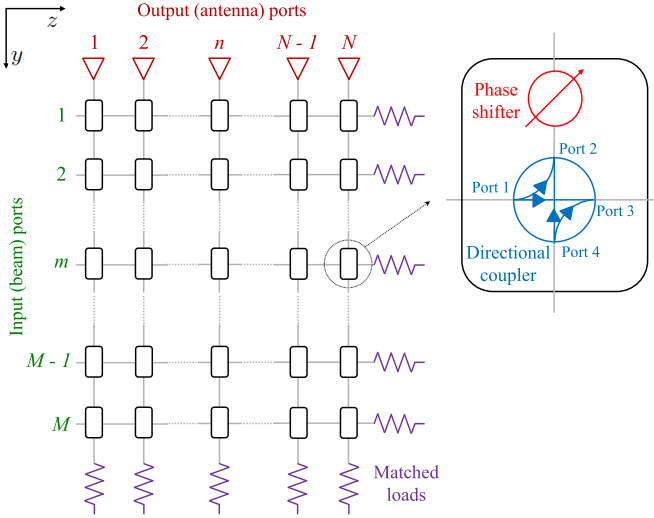


Fig. 1.  $M \times N$  Blass matrix.

wavelength. Consider, in particular, the  $M \times N$  synthesized excitation phases

$$\alpha_{mn} = \arg(a_{mn}), \quad m \in \mathcal{M}, \quad n \in \mathcal{N} \quad (2)$$

which allow  $R(\mathbf{a}_m; \theta)$  to point its main beam in the  $m$ th desired direction. The topic addressed in this work concerns the development of a simple Blass matrix design procedure that realizes the values in (2), which will be referred to as the desired phases from this point onward. It is worth emphasizing that the desired phases are not optimized during the proposed procedure; indeed, they are assumed to be known a priori. Similarly, the antenna array (number of elements, positions, and element type) is also assumed to be known. The proposed design method focuses solely on the Blass-based BFN architecture.

To this aim, we preliminarily introduce the general characteristics of a Blass matrix. It consists of  $N$  vertical and  $M$  horizontal lines interconnected through  $M \times N$  nodes, where each node comprises a directional coupler and a phase shifter (Fig. 1). The  $M$  desired beams determine the input terminals and thus the number of matrix rows, while the  $N$  antennas determine the output terminals and thus the number of matrix columns. Both vertical and horizontal lines are terminated by matched loads to avoid reflections of the incident waves. The power dissipated at these terminals necessarily reduces the overall system efficiency, which can be, however, maintained close to 90% [12]. When a generic  $m$ th desired beam must be produced, the wave injected into the corresponding port travels through all the  $N$  output ones. Along this path, the transmission coefficient  $T_{mn}$  describes the amplitude and phase of the signal injected at beam port  $m$  and arrived at antenna port  $n$ , which, from the array perspective, can be seen as the element excitation  $a_{mn}$  in (1). Therefore, the Blass matrix design requires the characterization of its  $M \times N$  nodes, that is, its  $M \times N$  coupling coefficients  $C_{mn}$  and phase shifts  $\phi_{mn}$ , to obtain proper  $T_{mn}$  values at the antenna terminals. Within this process, the critical aspect is just represented by the coupling coefficients, which can be different from each

other and identified by any numerical value. In fact, during the evaluation stage, these components may be optimized [15], but, in the subsequent fabrication stage, some coupling values might be difficult, or even impossible, to realize. This limitation, whose extent depends on the adopted technology, might finally prevent the actual implementation of the designed BFN. Thus, two basic choices are made in this study to foster the practical realizability of a planned structure. First, in agreement with [13], an identical directional coupler is adopted for all matrix nodes, hence considering

$$C_{mn} = C, \quad m \in \mathcal{M}, \quad n \in \mathcal{N}. \quad (3)$$

This common coupler is assumed to be lossless and characterized by good isolation, perfect matching, and full symmetry, thus its scattering matrix can be expressed as

$$S = \begin{bmatrix} 0 & \sqrt{1-C^2} & Ce^{-j\xi} & 0 \\ \sqrt{1-C^2} & 0 & 0 & Ce^{-j\xi} \\ Ce^{-j\xi} & 0 & 0 & \sqrt{1-C^2} \\ 0 & Ce^{-j\xi} & \sqrt{1-C^2} & 0 \end{bmatrix} \quad (4)$$

where  $\xi$  is the coupling phase between the input and coupled ports, and between the direct and isolated ports (Fig. 1). The choice of using an identical coupler also enables to express the transmission coefficients of the Blass matrix as the functions

$$T_{mn} = T_{mn}(C, \xi; \phi_{1n}, \dots, \phi_{mn}), \quad m \in \mathcal{M}, \quad n \in \mathcal{N} \quad (5)$$

where  $\phi_{mn}$  denotes the phase shift corresponding to node  $(m, n)$ . As a second basic choice,  $C$  and  $\xi$  are considered given, since the existing coupler design techniques usually focus on a limited set of values [28], [29], [30], typically corresponding to  $C \in \mathbb{C}$  and  $\xi \in \mathfrak{E}$ , with

$$\mathbb{C} = \left\{ \frac{1}{1000}, \frac{1}{100}, \frac{1}{10}, \frac{1}{2}, \frac{1}{\sqrt{2}} \right\} \quad (6a)$$

$$\mathfrak{E} = \left\{ -\pi, -\frac{\pi}{2}, \frac{\pi}{2}, \pi \right\}. \quad (6b)$$

The two choices imply that the amplitudes of the excitations are not directly controlled, but derived from the coupling values and the phase shifts. According to the scope of this study, the same choices enable the control of the beam pointing directions and, when required, of the possible null ones.

So, finally, the objective of this article is precisely the derivation of the  $M \times N$  phase shift values  $\phi_{mn}$  of the Blass matrix that allows one to satisfy the set of design equations

$$\arg(T_{mn}) = \alpha_{mn}, \quad m \in \mathcal{M}, \quad n \in \mathcal{N} \quad (7)$$

when the coupling parameters  $C$  and  $\xi$  in (5), and the  $M \times N$  desired phases  $\alpha_{mn}$  in (7) are given. The method developed to deal with this problem is presented in Section III.

### III. DESIGN PROCEDURE

In a Blass matrix, a wave traveling from an input port  $m$  to an output port  $n$  can take multiple paths, including the direct one and the spurious paths, which are present for  $m, n \geq 2$ . In the direct path, the wave travels along the  $m$ th row until it reaches the  $n$ th column and then turns to arrive at the  $n$ th antenna. In a spurious path, the wave still starts traveling

along the  $m$ th row, but turns before reaching the  $n$ th column, so arriving at the  $n$ th antenna only after multiple additional turns. Ignoring spurious paths is acceptable when considering large arrays with low coupling values. Conversely, it may result in poor approximations and inaccurate results [13] in the case of small arrays with high coupling values. Therefore, in the proposed design procedure, all possible paths are taken into account. Moreover, since only the direct path is present for  $m, n = 1$ , while spurious paths exist for  $m, n \geq 2$ , the procedure is divided into two main parts that correspond to the two sets of ports.

#### A. Ports $m, n = 1$

Let us consider the first input port ( $m = 1$ ), from which the wave can reach a generic output port  $n$  through the sole direct path. The corresponding transmission coefficient from each output port may be expressed, for  $m = 1$  and  $n \in \mathcal{N}$ , as

$$T_{1n} = C^{n-1} \sqrt{1 - C^2} \exp[-j(\phi_{1n} + \psi_{1n})] \quad (8)$$

where the second phase term is defined, for  $m \in \mathcal{M} \cup \{0\}$  and  $n \in \mathcal{N} \cup \{0\}$ , as

$$\psi_{mn} = (n - 1)(\xi + \delta_z) + (m - 1)(\xi + \delta_y). \quad (9)$$

Here,  $\delta_z$  and  $\delta_y$  are the given phase delays that account for the propagation along the sections joining consecutive couplers lying on the same row and column, respectively. In (9), the indexes  $n = 0$  and  $m = 0$  are included for mathematical purposes to improve the compactness of the formulas illustrated in the sequel. By substituting (8) into (7) and then solving for  $\phi_{1n}$ , one can obtain the searched phase shift values on the first row as

$$\phi_{1n} = -(\alpha_{1n} + \psi_{1n}), \quad n \in \mathcal{N}. \quad (10)$$

A similar approach may be adopted to address the first output port ( $n = 1$ ), which can be reached from a generic input port  $m$  still through the sole direct path. In this case, the corresponding transmission coefficient from each of the  $M$  input ports may be written, for  $n = 1$  and  $m \in \mathcal{M}$ , as

$$T_{m1} = C^{m-1} \sqrt{1 - C^2} \exp\left[-j\left(\sum_{i=1}^m \phi_{i1} + \psi_{m1}\right)\right]. \quad (11)$$

Since in an antenna array, the generated pattern does not depend on the absolute excitation phases, but on their relative phase shifts, the desired phase  $\alpha_{m1}$  of the first array element can always be set to zero for  $m \in \mathcal{M}$ . By imposing this choice to (10), the searched phase shift value on the first row and column becomes exactly

$$\phi_{11} = 0. \quad (12)$$

Substituting (11) into (7) with  $\alpha_{m1} = 0$  for  $m \in \mathcal{M} - \{1\}$  and using (12), the resulting set of equations can be solved in increasing order of  $m$  for the unknown  $\phi_{m1}$ . This provides the remaining  $M - 1$  searched phase shift values on the first column as

$$\phi_{m1} = \psi_{01}, \quad m \in \mathcal{M} - \{1\}. \quad (13)$$

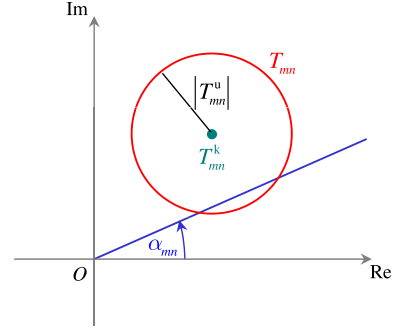


Fig. 2. Unknown phase shift evaluation.

#### B. Ports $m, n \geq 2$

The set of ports corresponding to  $m, n \geq 2$  is characterized by the existence of both direct and spurious paths. In fact, a wave traveling from port  $m$  to port  $n$ , for  $m \in \mathcal{M} - \{1\}$  and  $n \in \mathcal{N} - \{1\}$ , passes through

$$I_{mn} = \binom{n + m - 2}{m - 1} \quad (14)$$

different paths. Besides, whichever path the wave follows among the possible  $I_{mn}$  ones, it passes through  $m + n + 1$ -directional couplers and  $m$  phase shifters. The evaluation is carried out by iteratively proceeding element-wise row-by-row, starting with the nodes from  $(2, 2)$  to  $(2, N)$  and concluding with the nodes from  $(M, 2)$  to  $(M, N)$ . In this way, the estimation of an unknown  $\phi_{mn}$  value can rely on the phase shifts  $\phi_{ih}$  already calculated for  $i < m, h \in \mathcal{N}$  and  $i = m, h < n$ . This implies that all the  $I_{mn} - 1$  spurious paths are characterized by known phase shifters. Consequently, the transmission coefficient  $T_{mn}$ , for  $m \in \mathcal{M} - \{1\}$  and  $n \in \mathcal{N} - \{1\}$ , can be split into two parts as

$$T_{mn} = T_{mn}^k + T_{mn}^u \quad (15)$$

where  $T_{mn}^k$  is associated with the known spurious path contributions, while  $T_{mn}^u$  is associated with the unknown direct path contribution. This latter one, corresponding to a wave in transit through the unknown phase shifter  $\phi_{mn}$ , may be written, for  $m \in \mathcal{M} - \{1\}$  and  $n \in \mathcal{N} - \{1\}$ , as

$$T_{mn}^u = C^{n+m-2} \sqrt{1 - C^2} \exp[-j(\zeta_{mn} + \phi_{mn})] \quad (16)$$

where

$$\zeta_{mn} = \sum_{i=1}^{m-1} \phi_{in} + \psi_{mn} \quad (17)$$

is known from the previous calculations, and the modulus

$$|T_{mn}^u| = \sqrt{1 - C^2} C^{n+m-2} \quad (18)$$

is also known, being the directional coupler selected at the beginning of the procedure. A graphical interpretation in the complex plane of the resulting  $\phi_{mn}$  searching process may be inferred from Fig. 2. The figure shows the possible excitations with desired phase  $\alpha_{mn}$  (blue straight line) and the feasible  $T_{mn}$  values (red circumference) identified by the points lying at distance  $|T_{mn}^u|$  (black segment) from the center  $T_{mn}^k$  (green dot).

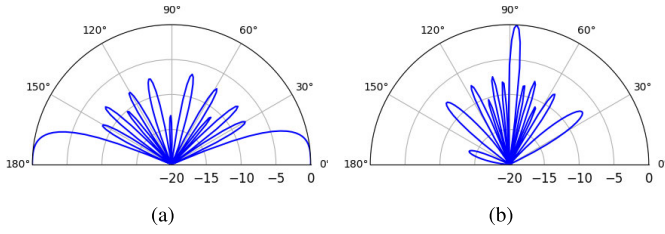


Fig. 3. Example 1—Generated patterns. (a)  $m = 1$ . (b)  $m = 2$ .

In particular, the design equation in (7) corresponding to  $\alpha_{mn}$  has a solution if at least one intersection point exists between the blue straight line and the red circumference [17]. From an algebraic perspective, the acceptable values for the phase shift can be determined by substituting (15), (16), and (18) into (7), and numerically solving the resulting equation for the unknown  $\phi_{mn}$

$$\arg\{T_{mn}^k + |T_{mn}^u| \exp[-j(\zeta_{mn} + \phi_{mn})]\} = \alpha_{mn}. \quad (19)$$

This equation can provide one, two, or no solutions. In the first two cases, the procedure can proceed to estimate the subsequent phase shift. When two solutions are acceptable, the one corresponding to the  $T_{mn}$  value further from the origin  $O$  is selected. If all the  $(M - 1) \times (N - 1)$  equations corresponding to  $m \in \mathcal{M} - \{1\}$  and  $n \in \mathcal{N} - \{1\}$  have a solution, all matrix nodes are characterized, and the procedure successfully terminates. Conversely, if (19) has no solution, which corresponds to the red circumference and the blue straight line in Fig. 2 having no intersections, the procedure must be interrupted. This possible outcome, which derives from adopting an identical coupler for all nodes, does not necessarily imply the unsolvability of the problem. Rather, it simply means that solutions cannot be obtained when the desired beams, and hence the  $M$  desired phase vectors  $\alpha_m = [\alpha_{m1}, \dots, \alpha_{mN}]$  for  $m \in \mathcal{M} - \{1\}$ , are imposed in that order. More precisely, since each phase shift  $\phi_{mn}$  depends on the previous  $T_{mn}^k$  value calculated during the process, the order in which the desired phase vectors are considered affects the final result and the feasibility of the procedure. To manage this situation, the phase vectors  $\alpha_1, \dots, \alpha_M$  are permuted until a feasible solution is obtained or all permutations are explored. The overall procedure is summarized in Algorithm 1. To speed up the process, when an unsolvable equation is encountered for  $\alpha_m$  at a certain permutation  $i$ , the  $(M - m)!$  permutations having the same starting point are not considered, since they would not lead to a successful design.

#### IV. RESULTS

The effectiveness of the developed procedure is investigated by presenting two numerical applications. The first one, discussed in Section IV-A, concerns a  $2 \times 10$  Blass BFN feeding an ALA of isotropic radiators, while the second one, illustrated in Section IV-B, involves a  $4 \times 4$  Blass matrix feeding an ULA of rectangular microstrip patches. The phase shifts evaluation algorithm is implemented in MATLAB on

#### Algorithm 1 Proposed Procedure

---

**Input:** ALA  $\rightarrow N, z_n, f_n(\theta), n \in \mathcal{N}$   
 Desired phase vectors  $\rightarrow M, \alpha_m, m \in \mathcal{M}$   
 Directional coupler  $\rightarrow C, \xi$   
 Blass matrix geometry  $\rightarrow \delta_x, \delta_y$

**Output:** Phase shifters  $\rightarrow \phi_{mn}, m \in \mathcal{M}, n \in \mathcal{N}$

- 1 Create matrix  $\Theta \in ]-\pi, \pi]^{M! \times M}$  of all possible permutations of desired phase vectors
- 2 Initialize  $m = 1, i = 1 - (M - m)!$
- 3 Set  $i = i + (M - m)!$
- 4 **if**  $i \leq M!$  **then**
  - 5 For permutation  $i$
  - 6 For  $n \in \mathcal{N}$  use (10) and (12) to derive  $\phi_{1n}$  // Row 1
  - 7 For  $m \in \mathcal{M}$  use (13) to derive  $\phi_{m1}$  // Column 1
  - 8 **while**  $m < M$  **do**
    - 9 Set  $n = 1$
    - 10  $m = m + 1$
    - 11 **while**  $n < N$  **do**
      - 12  $n = n + 1$
      - 13 Calculate  $T_{mn}^k$  // Transmission coefficient for spurious paths
      - 14 Use (18) to derive  $|T_{mn}^u|$  // Transmission coefficient modulus for direct path
      - 15 **if** (19) has solution **then**
        - 16 Evaluate  $\phi_{mn}$  // Phase shift
        - 17 **if**  $m = M$  and  $n = N$  **then**
          - 18 Blass matrix designed
      - 19 **else**
        - 20 go to line 3
  - 21 **else**
    - 22 Blass matrix designed

---

TABLE I  
EXAMPLE 1—ALA NORMALIZED ELEMENT POSITIONS

$n$	1	2	3	4	5	6	7	8	9	10
$z_n/\lambda$	0	0.5	1	2.5	4	5	6.5	8	8.5	9

a laptop equipped with an Intel<sup>1</sup> Core<sup>2</sup> i7-12800h CPU @ 2.40 GHz with 32 GB RAM.

##### A. Example 1

The first numerical example involves an ALA composed of  $N = 10$  isotropic elements, whose positions are specified in Table I. The ALA is required to radiate  $M = 2$  independent beams, with the first pointing direction at  $\theta_1 = 0^\circ$  and the second at  $\theta_2 = 87^\circ$ . Additionally, the first beam needs to have a null at  $\theta_n = \theta_2$ , corresponding to the direction of the second desired beam. The synthesis of the desired phases is realized

<sup>1</sup>Registered trademark.

<sup>2</sup>Trademarked.

TABLE II  
EXAMPLE 1—CALCULATED PHASE SHIFTS

Port	$\theta_m$	$n=1$	$n=2$	$n=3$	$n=4$	$n=5$	$n=6$	$n=7$	$n=8$	$n=9$	$n=10$
$m=1$	$0^\circ$ , with $\theta_n = 87^\circ$	$0^\circ$	$164.8^\circ$	$-0.5^\circ$	$167.9^\circ$	$-6.8^\circ$	$-9.8^\circ$	$177.0^\circ$	$-15.7^\circ$	$179.9^\circ$	$-16.1^\circ$
$m=2$	$87^\circ$	$0^\circ$	$-155.6^\circ$	$19.5^\circ$	$-121.3^\circ$	$82.6^\circ$	$104.4^\circ$	$-55.1^\circ$	$166.7^\circ$	$-20.0^\circ$	$-174.3^\circ$

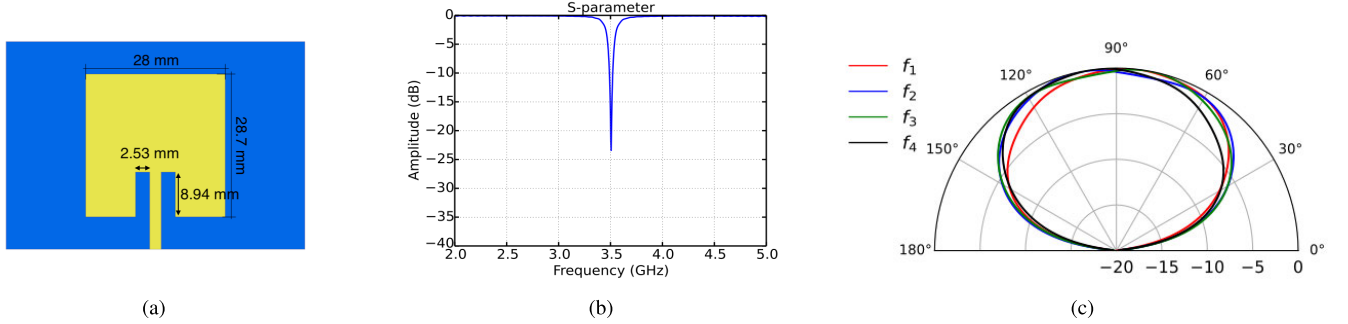


Fig. 4. Example 2—Designed patch. (a) Dimensions. (b) Return loss. (c) Element patterns.

by first selecting

$$\alpha_{mn} = -\frac{2\pi}{\lambda} z_n \cos \theta_m, \quad m \in \mathcal{M}, \quad n \in \mathcal{N} \quad (20)$$

and then modifying the  $\alpha_1$  vector according to the method in [31] to impose the required null in the first pattern. The input data for Algorithm 1 includes the parameters for the selected directional coupler ( $C = 1/10$  and  $\xi = \pi$ ) as well as the phase delays due to the joining sections ( $\delta_z = \delta_y = \pi$ ). It is worth noting that the feed-network architecture is assumed to be regular, despite the aperiodic positions of the elements, so that the phase delays due to the joining sections are constant. However, if an irregular design is adopted, it is straightforward to modify (9) to consider variable (but known) phase delays  $\delta_{zn}, \delta_{ym}$ .

The patterns shown in Fig. 3 are generated using the so derived  $\phi_{mn}$  values, which are reported in Table II and have been obtained at the first permutation in a CPU time of 6 ms. The figure demonstrates that the beams realized through the designed Blass matrix are oriented in agreement with the desired directions. Besides the satisfactory behavior of the proposed procedure, this first example further highlights its versatility, since the multibeam realization problem can be addressed in conjunction with null placement constraints using linear arrays (LAs) with a nonuniform geometry.

### B. Example 2

The second example is presented to evaluate the algorithm's performance in solving a practical problem. This problem is addressed through full-wave simulations and experimental measurements on a prototype fabricated using printed circuit board (PCB) technology. The application involves a ULA composed of  $N = 4$  rectangular microstrip patches, which are required to radiate  $M = 4$  independent beams at  $\theta_1 = 60^\circ$ ,  $\theta_2 = 85^\circ$ ,  $\theta_3 = 110^\circ$ , and  $\theta_4 = 140^\circ$ . The design frequency is set to 3.5 GHz, corresponding to the 5G C-band recently released for commercial use, which leads to a free-space

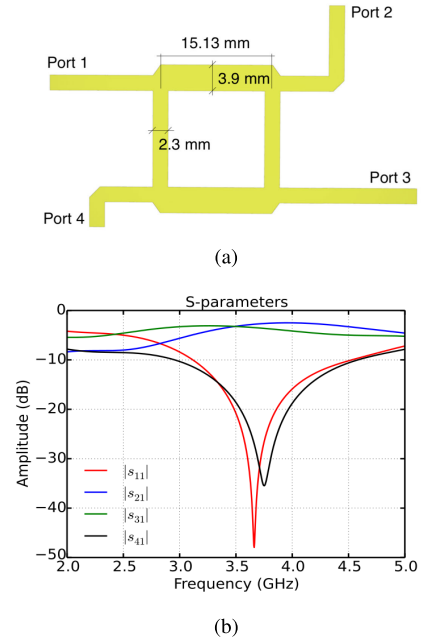


Fig. 5. Example 2—Designed coupler. (a) Dimensions. (b) S-parameters.

wavelength  $\lambda \cong 85.7$  mm and a guided wavelength  $\lambda_g \cong 57.8$  mm. For the PCB, a Rogers 5880 substrate with a dielectric constant  $\epsilon_r = 2.2$ , a substrate thickness  $\chi = 0.8$  mm, and a metallization thickness  $\zeta = 3.5 \mu\text{m}$  is chosen.

Starting with these preliminary data, the basic components, namely the patches and the directional coupler, are designed, simulated, and optimized using CST Studio Suite [32]. The dimensions of the antenna element obtained from the simulation are presented in Fig. 4(a), while Fig. 4(b) shows that the obtained antenna element has good matching at the design frequency. Four of these radiators are organized to form the ULA with an interelement (center-to-center) distance  $d = 50$  mm. The resulting single-element patterns  $f_n(\theta)$  ( $n \in \mathcal{N}$ ), which account for the mutual coupling effects, are

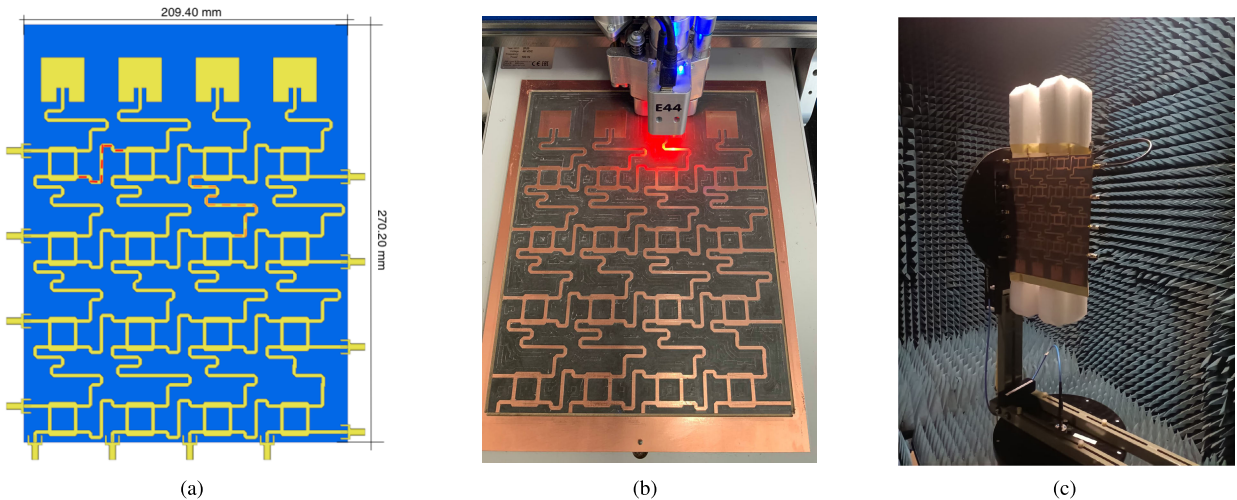


Fig. 6. Example 2—Developed structure. (a) Design. (b) Milling prototype. (c) Test in an anechoic chamber.

TABLE III  
EXAMPLE 2—CALCULATED PHASE SHIFTS

Port	Beam	$\theta_{m'}$	$n=1$	$n=2$	$n=3$	$n=4$
$m=1$	$m'=1$	$60^\circ$	$0^\circ$	$109.1^\circ$	$-141.7^\circ$	$-32.6^\circ$
$m=2$	$m'=3$	$110^\circ$	$-90.0^\circ$	$-90.0^\circ$	$84.2^\circ$	$-95.7^\circ$
$m=3$	$m'=2$	$85^\circ$	$-90.0^\circ$	$87.5^\circ$	$92.4^\circ$	$90.0^\circ$
$m=4$	$m'=4$	$140^\circ$	$-90.0^\circ$	$95.1^\circ$	$-85.9^\circ$	$148.1^\circ$

derived using the method described in [33] and are reported in Fig. 4(c). The desired phases are obtained by (20) with  $z_n = (n-1)d$  for  $n \in \mathcal{N}$ .

With the ULA and desired phases characterized, the next step is to design the directional coupler. In particular, a branch line coupler with parameters  $C = 1/\sqrt{2}$  and  $\xi = \pi/2$  is developed using the technique discussed in [34] and subsequently optimized by CST, resulting in the structure illustrated in Fig. 5(a). The  $S$ -parameters reported in Fig. 5(b) confirm its satisfactory performance at the design frequency. In fact, the reflection coefficient  $|s_{11}|$  and the isolation  $|s_{14}|$  are both low, indicating good matching at the input port and fine decoupling at the isolated one. Additionally, the  $|s_{21}|$  and  $|s_{31}|$  values are both very close to  $-3$  dB, confirming that the power is equally divided between the direct and the coupled port, as desired. The final input quantity required by the proposed procedure is represented by the phase delays determined by the sections connecting consecutive directional couplers on the rows and columns. In both cases, these sections are realized through microstrip lines of length exactly equal to the guided wavelength  $\lambda_g$ , corresponding to phase delays  $\delta_z = \delta_y = 2\pi$ .

With the insertion of the input parameters characterizing the components (patches, desired phases, couplers, and phase delays) into Algorithm 1, the calculation of the necessary phase shifts to complete the Blass matrix design can be performed. The resulting values, obtained for permutation  $i = 3$  in a CPU time of 20 ms, are reported in Table III. Note that, differently from the previous example, the pointing

directions are not activated by the input (beam) ports in the original increasing order. For instance, while the first desired beam corresponding to  $\theta_1 = 60^\circ$  is activated by port  $m = 1$ , the second one corresponding to  $\theta_2 = 85^\circ$  is instead activated by port  $m = 3$ . This is due to the algorithm permutations that became necessary to obtain a complete solution, since, clearly, in this second example, the first permutation has not been able to achieve a successful result. On the PCB, each estimated  $\phi_{mn}$  value is realized by a meander line of proper length that connects a coupler on the first row with the respective patch or two consecutive couplers lying on the same column.

The phase shift implementation completes the design of the Blass matrix, which can be combined with the other components to finally obtain the array-BFN system reported in Fig. 6(a). For a more immediate identification of the different parts of the structure, the figure highlights the phase delay  $\delta_z$  between the first two couplers on the first row (red dashed line), and the phase shift  $\phi_{23}$  joined with the phase delay  $\delta_y$  between the first two couplers on the third column (orange dashed line). This system is first implemented in CST to evaluate its radiation patterns through full-wave simulation and subsequently physically built to validate these patterns through experimental measurements. To this aim, an LPKF ProtoMat E44 milling machine is adopted to realize the prototype in Fig. 6(b) and (c), which, respectively, illustrate the final stages of the manufacturing process and the subsequent installation in an anechoic chamber.

The matching of the developed Blass matrix at the four input ports may be observed from Fig. 7, which reports the corresponding reflection coefficients simulated by CST and measured using a Rohde&Schwarz ZVA40 10 MHz–40 GHz vector network analyzer. Fig. 8 illustrates the simulated and measured far-field patterns for the four required beams. In particular, this figure shows that, except for a few degrees of drift, the experimentally derived pointing directions are in very good agreement with the desired ones. Despite the fabrication tolerances, the measured patterns closely approach the simulated ones in the main lobe regions. Finally, it is worth noting that the simulated efficiencies at the four input ports are

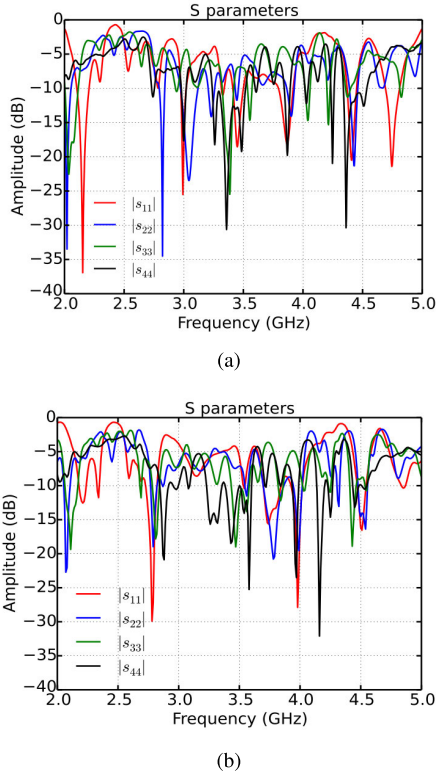


Fig. 7. Example 2—Reflection coefficients. (a) Simulated. (b) Measured.

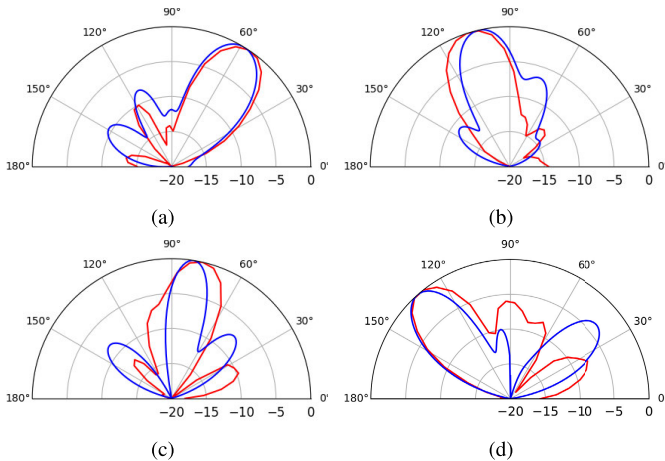


Fig. 8. Example 2—Generated patterns. (a)  $m = 1$ . (b)  $m = 2$ . (c)  $m = 3$ . (d)  $m = 4$ . — simulated — measured.

satisfactory, being, 71%, 68%, 63%, and 61%, respectively. These values are basically in agreement with those provided in [15] and [35]. These practical results demonstrate besides the fast response of the developed algorithm, the reliability of the estimated phase shifts for the actual realization of simple Blass BFNs that can support multibeam functionalities.

### C. Convergence Characteristics

In both the presented examples, the algorithm provides a satisfactory solution. However, as mentioned in Section III, the choice of having the same coupler for all the matrix nodes simplifies the BFN structure at the expense of flexibility.

In particular, the algorithm might fail to provide a solution for some sets of desired phases and coupling values. Hence, in this section, to provide a clearer view of the practical usefulness of the algorithm, a random evaluation of its convergence to an acceptable solution is carried out. More precisely, a large number of random trials is performed and the success probability  $p_s$  is evaluated for different values of the design parameters  $N$ ,  $M$ , and  $C$ . Blass matrices having  $N = 4, 8, 16, 32$  and  $M = 2, 3, \dots, 8$  are considered for values of  $C \in \mathbf{C}$ , where the set  $\mathbf{C}$  is defined in (6a). For each combination of  $N$ ,  $M$ , and  $C$ , 1000 sets of pointing directions are randomly generated in the interval  $[0, \pi]$ . Subsequently, the  $M \times N$  desired phases are obtained according to (20), assuming an ULA with  $d = \lambda/2$ . The remaining parameters are set as  $\xi = \pi/2$  and  $\delta_y = \delta_z = 2\pi$ .

The obtained results show that, for the three lowest values of  $C$ , that is,  $C = 10^{-3}, 10^{-2}, 10^{-1}$ , the algorithm always provides a solution, that is,  $p_s = 1$  for all  $N, M$  choices. When  $C = 1/2$  is selected and all the considered  $M$  values are explored, the success probability remains equal to unity for  $N = 4$ , lies between 0.67 and 0.98 for  $N = 8$ , while it approaches zero for  $N = 16, 32$ . Finally, in the case  $C = 1/\sqrt{2}$ , the method provides solutions just for  $N = 4$ , with  $p_s \in [0.21, 0.36]$ . On the other hand, in this case, the maximum radiation efficiency attains its best value corresponding to 0.94. Moreover, the case  $C = 1/2$  provides a quite satisfactory maximum efficiency close to 0.90, while, as expected, for smaller coupling values the efficiency decreases, being approximately equal to 0.28 when  $C = 1/10$ . In general, this random investigation of the convergence confirms that the algorithm presents some limitations just for high values of the coupling coefficient, while it always provides a solution in the main part of the  $C$  domain. This confirms the applicability of the developed method to many BFN design problems relying on the Blass network and requiring simplicity of implementation.

## V. CONCLUSION

In conclusion, a novel Blass matrix design strategy has been proposed to enable ALAs to generate multiple independent beams. The technique relies on the adoption of an identical directional coupler and an iterative procedure for determining the phase shift values. The method has been successfully applied to antenna pattern generation problems, allowing for the radiation of arbitrarily oriented beams with null constraints while maintaining very low CPU times and ensuring accurate beam pointing. As a proof-of-concept, the feasibility of the proposed approach has been experimentally verified through the fabrication of an array-BFN system using PCB technology, providing a comprehensive and cost-effective solution for multibeam antenna design.

## REFERENCES

- [1] F. Braun. (Dec. 1909). *Electrical Oscillations and Wireless Telegraphy*. [Online]. Available: [http://ip.cadence.com/uploads/112/ConnX\\_BBE64-pdf](http://ip.cadence.com/uploads/112/ConnX_BBE64-pdf)
- [2] L. C. Godara, "Application of antenna arrays to mobile communications, Part II: Beam forming and direction-of-arrival considerations," *Proc. IEEE*, vol. 85, no. 8, pp. 1193–1245, Aug. 1997.



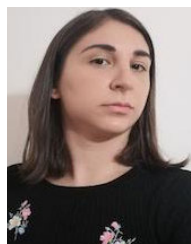
- [3] R. L. Haupt and Y. Rahmat-Samii, "Antenna array developments: A perspective on the past, present and future," *IEEE Antennas Propag. Mag.*, vol. 57, no. 1, pp. 86–96, Feb. 2015.
- [4] W. Roh et al., "Millimeter-wave beamforming as an enabling technology for 5G cellular communications: Theoretical feasibility and prototype results," *IEEE Commun. Mag.*, vol. 52, no. 2, pp. 106–113, Feb. 2014.
- [5] M. Giordani and M. Zorzi, "Non-terrestrial networks in the 6G era: Challenges and opportunities," *IEEE Netw.*, vol. 35, no. 2, pp. 244–251, Mar. 2021.
- [6] W. Hong et al., "Multibeam antenna technologies for 5G wireless communications," *IEEE Trans. Antennas Propag.*, vol. 65, no. 12, pp. 6231–6249, Dec. 2017.
- [7] Z. Xiao et al., "Antenna array enabled space/air/ground communications and networking for 6G," *IEEE J. Sel. Areas Commun.*, vol. 40, no. 10, pp. 2773–2804, Oct. 2022.
- [8] M. Younis, C. Fischer, and W. Wiesbeck, "Digital beamforming in SAR systems," *IEEE Trans. Geosci. Remote Sens.*, vol. 41, no. 7, pp. 1735–1739, Jul. 2003.
- [9] V. Venkateswaran and A.-J. van der Veen, "Analog beamforming in MIMO communications with phase shift networks and online channel estimation," *IEEE Trans. Signal Process.*, vol. 58, no. 8, pp. 4131–4143, Aug. 2010.
- [10] S. Han, Z. Xu, and C. Rowell, "Large-scale antenna systems with hybrid analog and digital beamforming for millimeter wave 5G," *IEEE Commun. Mag.*, vol. 53, no. 1, pp. 186–194, Jan. 2015.
- [11] Y. J. Guo, M. Ansari, and N. J. G. Fonseca, "Circuit type multiple beamforming networks for antenna arrays in 5G and 6G terrestrial and non-terrestrial networks," *IEEE J. Microw.*, vol. 1, no. 3, pp. 704–722, Jul. 2021.
- [12] J. Blass, "Multidirectional antenna—A new approach to stacked beams," in *Proc. IRE Int. Conv. Rec.*, vol. 8, Mar. 1966, pp. 48–50.
- [13] F. Casini, R. V. Gatti, L. Marcaccioli, and R. Sorrentino, "A novel design method for Blass matrix beam-forming networks," in *Proc. Eur. Microw. Conf.*, Oct. 2007, pp. 1511–1514.
- [14] W. R. Jones and E. C. DuFort, "On the design of optimum dual-series feed networks," *IEEE Trans. Microw. Theory Techn.*, vol. MTT-19, no. 5, pp. 451–458, May 1971.
- [15] S. Mosca, F. Bilotti, A. Toscano, and L. Vegni, "A novel design method for Blass matrix beam-forming networks," *IEEE Trans. Antennas Propag.*, vol. 50, no. 2, pp. 225–232, Feb. 2002.
- [16] C. A. Guo, Y. J. Guo, H. Zhu, W. Ni, and J. Yuan, "Optimization of multibeam antennas employing generalized joined coupler matrix," *IEEE Trans. Antennas Propag.*, vol. 71, no. 1, pp. 215–224, Jan. 2023.
- [17] G. M. Schettino, F. Babich, and G. Buttazzoni, "Design of a simple feeding network for 5G multidirectional antennas," in *Proc. IEEE 94th Veh. Technol. Conf.*, Sep. 2021, pp. 1–5.
- [18] G. Buttazzoni et al., "A beamforming network for 5G/6G multibeam antennas using the PCB technology," in *Proc. 17th Eur. Conf. Antennas Propag. (EuCAP)*, Mar. 2023, pp. 1–5.
- [19] W. Y. Lim and K. K. Chan, "Generation of multiple simultaneous beams with a modified Blass matrix," in *Proc. Asia Pacific Microw. Conf.*, Dec. 2009, pp. 1557–1560.
- [20] N. J. G. Fonseca, "Printed S-band  $4 \times 4$  Nolen matrix for multiple beam antenna applications," *IEEE Trans. Antennas Propag.*, vol. 57, no. 6, pp. 1673–1678, Jun. 2009.
- [21] T. Djerafi, N. J. G. Fonseca, and K. Wu, "Broadband substrate integrated waveguide  $4 \times 4$  Nolen matrix based on coupler delay compensation," *IEEE Trans. Microw. Theory Techn.*, vol. 59, no. 7, pp. 1740–1745, Jul. 2011.
- [22] J. Allen, "A theoretical limitation on the formation of lossless multiple beams in linear arrays," *IRE Trans. Antennas Propag.*, vol. AP-9, no. 4, pp. 350–352, Jul. 1961.
- [23] W. P. Delaney, "An RF multiple beam-forming technique," *IRE Trans. Mil. Electron.*, vol. MIL-6, no. 2, pp. 179–186, Apr. 1962.
- [24] H. Moody, "The systematic design of the Butler matrix," *IEEE Trans. Antennas Propag.*, vol. AP-12, no. 6, pp. 786–788, Nov. 1964.
- [25] W. C. Cummings, "Multiple beam forming networks," Lincoln Lab., Massachusetts Inst. Technol., Lexington, MA, USA, Tech. Rep. A056904, Apr. 1978. [Online]. Available: <https://apps.dtic.mil/sti/pdfs/ADA056904.pdf>
- [26] N. J. G. Fonseca, "Discussion on reciprocity, unitary matrix, and lossless multiple beam forming networks," *Int. J. Antennas Propag.*, vol. 2015, pp. 1–9, Jan. 2015.
- [27] J. Shelton and K. Kelleher, "Multiple beams from linear arrays," *IRE Trans. Antennas Propag.*, vol. 9, no. 2, pp. 154–161, Mar. 1961.
- [28] J.-C. Chiu, J.-M. Lin, M.-P. Houn, and Y.-H. Wang, "A PCB-compatible 3-dB coupler using microstrip-to-CPW via-hole transitions," *IEEE Microw. Wireless Compon. Lett.*, vol. 16, no. 6, pp. 369–371, Jun. 2006.
- [29] H. Ghorbaninejad and R. Heydarian, "New design of waveguide directional coupler using genetic algorithm," *IEEE Microw. Wireless Compon. Lett.*, vol. 26, no. 2, pp. 86–88, Feb. 2016.
- [30] M. M. M. Ali, O. M. Haraz, I. Afifi, A.-R. Sebak, and T. A. Denidni, "Ultra-wideband compact millimeter-wave printed ridge gap waveguide directional couplers for 5G applications," *IEEE Access*, vol. 10, pp. 90706–90714, 2022.
- [31] R. Vescovo, "Null synthesis by phase control for antenna arrays," *Electron. Lett.*, vol. 36, no. 33, pp. 198–199, 2000.
- [32] Dassault Systèmes Simulia. *CST Computer Simulation Technology, Microwave Studio Suite*. Accessed: Sep. 6, 2023. [Online]. Available: <http://www.cst.com/>
- [33] R. Vescovo, "Null formation with excitation constraints in the pattern synthesis for circular arrays of antennas," *Electromagnetics*, vol. 21, no. 3, pp. 213–230, Apr. 2001.
- [34] D. M. Pozar, *Microwave Engineering*. New York, NY, USA: Wiley, 2011.
- [35] C. A. Guo and Y. J. Guo, "A general approach for synthesizing multibeam antenna arrays employing generalized joined coupler matrix," *IEEE Trans. Antennas Propag.*, vol. 70, no. 9, pp. 7556–7564, Sep. 2022.



**Giulia Buttazzoni** (Senior Member, IEEE) received the M.Sc. degree (summa cum laude) in telecommunication engineering and the Ph.D. degree in information engineering from the University of Trieste, Trieste, Italy, in 2008 and 2013, respectively.

In 2014, she joined the Department of Engineering and Architecture (DIA) of the University of Trieste, where she is currently an Associate Professor in electromagnetic fields and antennas. Her main research activity concerns antenna array synthesis techniques and numerical methods for electromagnetic fields.

Dr. Buttazzoni is a member of the Italian Electromagnetics Society (SIEM) and the National Inter-University Consortium for Telecommunications (CNIT).



**Elena Marongiu** (Student Member, IEEE) received the B.Sc. degree in electrical and electronic engineering and the M.Sc. degree in telecommunications engineering from the University of Cagliari, Cagliari, Italy, in 2016 and 2019, respectively.

In 2020, she collaborated with the Italian Space Agency (ASI) on the Sardinia Deep Space Antenna (SDSA) optical configuration and radio telescope development in the X/K/Ka bands for near and deep space applications. Currently, she is the Ph.D. Student in electronic and computer engineering with

the University of Cagliari. Her research interests concern the modeling, analysis, and characterization of antennas, with specific reference to the design of microstrip antennas for radio-astronomical and 5G wearable devices.



**Alessandro Fanti** (Senior Member, IEEE) received the M.Sc. degree in electronic engineering and the Ph.D. degree in electronic engineering and computer science from the University of Cagliari, Cagliari, Italy, in 2006 and 2012, respectively.

From 2013 to 2016, he was a Post-Doctoral Fellow of the Electromagnetic Group, University of Cagliari, where he is currently an Assistant Professor. He has authored/coauthored 57 articles in international journals. His research interests include the use of numerical techniques for modes computation of guiding structures, optimization, analysis, and design of waveguide slot arrays and patch antennas, radio propagation in urban environments, modeling of bioelectromagnetic phenomena, and microwave exposure systems for biotechnology and bioagriculture.

Dr. Fanti is a member of IEEE Antennas and Propagation Society, the Italian Electromagnetics Society (SIEM), the National Inter-University Consortium for Telecommunications (CNIT), and the Interuniversity Center for the Interaction Between Electromagnetic Fields and Biosystems. He is an Associate Editor for the IEEE JOURNAL OF ELECTROMAGNETICS, RF AND MICROWAVES IN MEDICINE AND BIOLOGY. Since 2020, he has been a Principal Investigator of the IAPC Project, funded with €5 million by the Italian Ministry of Economic Development (MISE), within the AGRIFOOD PON I&C 2014-2020 (CUP: B21B1900064008 COR: 1406652).



**Andrea Melis** received the B.Sc. degree in biomedical engineering from the University of Cagliari, Cagliari, Italy, in 2017.

He worked as an Assistant Researcher with the University of Cagliari. His research interests include EM modeling and development of RF coils at low and high frequencies, especially for MRI at high field, the design and realization of wireless sensor network (WSN) systems for the monitoring of industrial processes, such as bread manufacturing and intelligent transportation systems.



**Nicola Curreli** (Member, IEEE) received the M.Sc. degree from the University of Genoa, Genoa, Italy, in 2016, and the Ph.D. degree in electronic engineering from the University of Cagliari, Cagliari, Italy and the Italian Institute of Technology—IIT, Genoa, in 2020.

After completing the Ph.D. degree, he held a Fellow position with Graphene Laboratories—IIT, where he contributed to the Graphene Core 2 Project as part of the Graphene Flagship initiative. In 2019, he was a Visiting Researcher with the Physics and

Mechanical Engineering Departments, Columbia University, New York City, NY, USA, as part of the Marie Skłodowska-Curie RISE Action “SONAR H2020.” Between 2022 and 2023, he was a Visiting Researcher with the Molecular Foundry at Lawrence Berkeley National Laboratory, Berkeley, CA, USA. Currently, he is a Researcher with the Functional Nanosystems—IIT. Since 2023, he has been a recipient of the Marie Skłodowska-Curie Global Fellowship “2DTWIST.” The fellowship is in collaboration with the Transport at Nanoscale Interfaces Laboratory at Swiss Federal Laboratories for Materials Science and Technology (EMPA) in Switzerland. His research interests include the study of low-dimensional materials, their characterization, and their application in the field of photonics, and the design, implementation, and analysis of linear and nonlinear integrated optical, microwave devices, and antennas.

Dr. Curreli received the Young Scientists Award at the General Assembly and Scientific Symposium of URSI in 2022. He is also a member of the Topical Advisory Panel of Photonics and is an Academic Editor for the *Journal of Nanotechnology* and the *International Journal of Optics*. He is a part of the Committee of the Young Professionals Affinity Group of IEEE R8 Italy Section.



**Santi Concetto Pavone** (Senior Member, IEEE) was born in Patti (ME), Italy, in 1988. He received the B.Sc. and M.Sc. degrees (summa cum laude) in electronics engineering from the University of Messina, Messina, Italy, in 2010 and 2012, respectively, and the Ph.D. degree (with the additional label of “Doctor Europaeus”) in information engineering and science (electromagnetics engineering) from the University of Siena, Siena, Italy, in 2015.

He was a Visiting Ph.D. Student with the Institut d’Electronique et de Telecommunications de Rennes (IETR), Université de Rennes 1, Rennes, France, for five months, in 2015. From 2016 to July 2019, he was an Associate Researcher with the Laboratory of Applied Electromagnetics, University of Siena. Since August 2019, he has been an Assistant Professor with the Department of Electrical, Electronics, and Information Engineering (DIEEI), University of Catania, Catania, Italy. His current research interests include fundamental electromagnetic theory, radar design at millimeter waves, high-frequency techniques, focusing systems, nondiffractive localized pulses, and leaky-wave reconfigurable antennas based on liquid crystals.

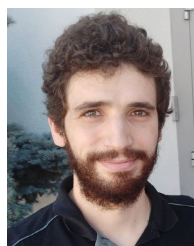
Dr. Pavone was a recipient of the European Science Foundation (ESF) Research Networking Program NEWFOCUS Scholarship in 2015 and the IEEE Antennas and Propagation Society Student Award and Chapter of the Central-Southern Italy in 2014. He was the Best Paper Award (BPA) Finalist and BPA co-recipient in electromagnetics and antenna theory at EuCAP’17 and EuCAP’18, respectively, and a recipient of the Young Scientist Award (YSA) at the 2019 PIER Symposium. He serves as an Associate Editor for IEEE ACCESS and as a Referee for the IEEE TRANSACTIONS ON ANTENNAS AND PROPAGATION.



**Gino Sorbello** (Member, IEEE) received the M.Sc. degree (cum laude) in electronics engineering from the University of Catania, Catania, Italy, in 1996, and the Ph.D. degree in electronics and communications engineering from the Polytechnic Institute of Milan, Milan, Italy, in 2000.

He became an Assistant Professor of Electromagnetic Fields with the University of Catania, in 2002. Since 2014, he has been an Associate Professor of Electromagnetic Fields with the Department of Electric, Electronics, and Computer Engineering, University of Catania. His current research interests include single-mode solid-state waveguide lasers and amplifiers, integrated optics, the development of planar antennas and ultrawideband compact antennas, and the study of microwave devices and computational electromagnetism with a special interest in RF–plasma interactions and particle accelerators.

Dr. Sorbello has been a member of INFN-LNS and collaborates with the Ion Sources and Plasma Physics Group, since 2012.



**Giovanni Maria Schettino** received the B.Sc. and M.Sc. degrees in computer and electronic engineering from the University of Trieste, Trieste, Italy, in 2018 and 2020, respectively.

From 2021 to 2022, he worked for u-blox as an RF Design Engineer and since August 2022, he is employed at Leonardo as an Avionic Operator. His research interests involve the design and simulation of microstrip antenna array feeding networks.



**Francesca Vatta** (Member, IEEE) received the M.Sc. degree in electronic engineering and the Ph.D. degree in telecommunications from the University of Trieste, Trieste, Italy, in 1992 and 1998, respectively.

She joined the Department of Engineering and Architecture (DIA) of the University of Trieste in 1999, where she is an Assistant Professor of Information Theory and Error-Control Coding. Starting in 2002 and 2005, she has been a Visiting Scholar, respectively, at Notre Dame University, Notre Dame, IN, USA, cooperating with the Coding Theory Research Group (RG) under the guidance of Prof. D.J. Costello, Jr., and at Ulm University, Ulm, Germany, cooperating with the telecommunications and applied information Theory RG under the guidance of Prof. M. Bossert. She is the author/coauthor of more than 100 papers published in international journals and conference proceedings. Her current research interests are in the area of channel coding concerning, in particular, the analysis and design of capacity-achieving codes.



**Fulvio Babich** (Senior Member, IEEE) received the M.Sc. degree (summa cum laude) in electrical engineering from the University of Trieste, Trieste, Italy, in July 1984.

After graduation, he was with Telettra at the Research and Development Laboratories, where he was engaged in optical fiber communications. Then he joined Zeltron as a Communication System Engineer, responsible for the activities within the ESPRIT program. In 1992, he joined the Department of Engineering and Architecture (DIA) of the University of Trieste, where he is a Full Professor of Digital Communications and Wireless Networks. His current research interests are in the field of wireless networks and millimeter-wave communications. He is involved in channel modeling, multiple access techniques, channel coding, error control techniques, and cross-layer design.

Dr. Babich is a member of the Board of National Telecommunications and Information Theory Group (GTTI), and he was a member of the Directive Board of the National Inter-University Consortium for Telecommunications (CNIT) and Coordinator of the Ph.D. Board in Industrial and Information Engineering of the University of Trieste.



**Massimiliano Comisso** (Member, IEEE) received the M.Sc. degree in electronic engineering and the Ph.D. degree in information engineering from the University of Trieste, Trieste, Italy, in 2003 and 2007, respectively.

He worked for Alcatel on Dense Wavelength Division Multiplexin (DWDM) optical systems and with Danieli Automation on electromagnetic Non Destructive Examination (NDE) modeling. Currently, he is an Associate Professor in Communication Networks and Waveguide/Optical Systems at the Department of Engineering and Architecture (DIA) of the University of Trieste. He is the author/coauthor of more than 100 international scientific papers and serves as a referee/TPC Member for several IEEE journals and conferences. His research interests involve antenna array synthesis, small antennas, millimeter-wave communications, and distributed wireless networks.

He has been the Best Student Paper Award (BPA) Finalist at IEEE GLOBECOM'06 and received the BPA at IEEE CAMAD'09.